JOURNAL OF MAGNETIC RESONANCE **131,** 144–147 (1998)
ARTICLE NO. MN971341

QCPMG-MAS NMR of Half-Integer Quadrupolar Nuclei

Flemming H. Larsen,*[,1] Hans J. Jakobsen,* Paul D. Ellis,† and Niels Chr. Nielsen*[,2]

*Instrument Centre for Solid-State NMR Spectroscopy, Department of Chemistry, University of Aarhus, DK-8000 Aarhus C, Denmark; and †Environmental Molecular Sciences Laboratory, Pacific Northwest National Laboratory, Richland, Washington 99352

Received May 27, 1997; revised November 14, 1997

By combination of fast magic-angle spinning (MAS) and detection of the free-induction decay during a rotor-synchronized quadrupolar Carr–Purcell–Meiboom–Gill (QCPMG) train of refocusing pulses, the sensitivity of quadrupolar-echo MAS NMR spectra for the central transition of half-integer quadrupolar nuclei exhibiting large quadrupolar couplings may be significantly enhanced. Enhancements by an order of magnitude may easily be realized while maintaining information about the anisotropic interactions. In the present study the so-called QCPMG-MAS experiment is demonstrated experimentally and by numerical simulations for the two ^{87}Rb sites in Rb_2SO_4. © 1998 Academic Press

Considerable interest in unraveling the combined effect of different anisotropic nuclear spin interactions in solid-state NMR spectroscopy has characterized the development of new experimental methods in recent years. In spectra of quadrupolar ($I > \frac{1}{2}$) nuclei the combined effect of the quadrupole coupling and chemical shielding interaction may appear. Both of these interactions reflect the local electronic environment of the quadrupolar nucleus. This situation has created renewed interest in the development of new and improved experimental and numerical methods for accurate determination of magnitudes and relative orientation for the two interactions, in particular for powders. For weak quadrupolar couplings ($C_Q/(2I - 1) < 0.5$ MHz, where C_Q is the quadrupole coupling constant) accurate parameters characterizing the two tensors may be obtained from one-pulse magic-angle spinning (MAS) NMR spectra of powders with special attention being paid to, e.g., symmetric excitation/detection of all transitions and highly stabilized spinning speed (*1, 2*). In the case of stronger quadrupole coupling (0.5 MHz $< C_Q/(2I - 1) < 5$ MHz) similar information may be obtained from the second-order quadrupolar-broadened central ($\frac{1}{2}$, $-\frac{1}{2}$) transition for half-integer quadrupolar nuclei in static powder (*3–6*) or MAS (*7, 8*) experiments. For larger quadrupolar couplings second-order broadening for the central transition on the order of hundreds of kilohertz generally reduces the spectral sensitivity.

We recently introduced the QCPMG experiment, i.e., the quadrupolar version (*9, 10*) of the Carr–Purcell–Meiboom–Gill (CPMG) (*11, 12*) experiment, as a means to increase the sensitivity of quadrupolar-echo (QE) spectra (*13–15*) for static powders. Increases in sensitivity by an order of magnitude have been observed while maintaining information about magnitudes and relative orientation of chemical shielding and quadrupole coupling tensors (*16*). Previously, this experiment has been used to distinguish inhomogeneous from homogeneous interactions in solid-state NMR (*9, 10, 17–25*), where the latter category include homonuclear dipolar coupling and molecular dynamics. For broad powder patterns induced by inhomogeneous second-order quadrupolar coupling, it should be possible to further improve the sensitivity and resolution by combining the QCPMG experiment with MAS. The obvious reason is that the second-order quadrupolar interaction is partially averaged by MAS—for infinitely fast spinning the width of the central transition lineshape is reduced by a factor of $72(1 + \eta_Q/6)^2/(7(\eta_Q^2 + 22\eta_Q + 25))$ (ranging from 0.29 to 0.41), where η_Q is the asymmetry parameter of the quadrupole coupling tensor (*26*). To exploit this possibility, this Communication introduces the so-called QCPMG-MAS experiment as a method for improving the sensitivity of MAS NMR of half-integer quadrupolar nuclei while retaining information about the tensors for the anisotropic interactions.

Figure 1 shows the timing diagram of the QCPMG-MAS pulse sequence. The pulse sequence consist of three basic elements. Part A is a standard rotor-synchronized solid echo (*13–15*) through which the decaying part of the initial spin echo is acquired to form the first part of the free-induction decay (FID). Part B represents the QCPMG part of the pulse sequence which through interrupted sampling appends the full spin-echo envelopes generated by the train of M refocusing π pulses to the FID. Finally, part C extends the sampling period to allow full decay of the FID. To ensure coincidence of rotary and spin echoes (i.e., an integral number of rotor periods per spin-echo period) the pulse sequence must be rotor synchronized. This is accomplished using $\tau_1 = \tau_r -$

[1] Present address: Environmental Molecular Sciences Laboratory, Pacific Northwest National Laboratory, Richland, WA 99352.

[2] To whom correspondence should be addressed.

1090-7807/98 $25.00

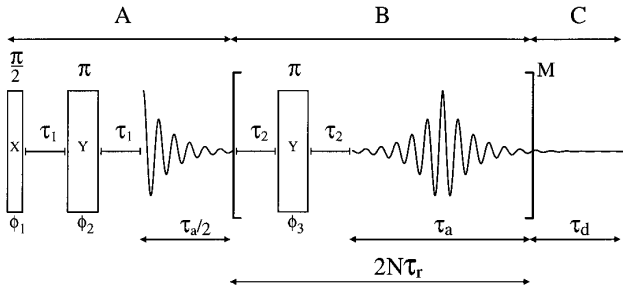

FIG. 1. Timing scheme of the QCPMG-MAS pulse sequence for sensitivity-enhanced QE-MAS NMR of nuclei exhibiting large anisotropic interactions. Following an initial solid echo with sampling of the decaying part of the echo (A), the remaining part of the free-induction decay (FID) is sampled during a rotor-synchronized train of M π pulses (B) ending with an extended acquisition period (C) ensuring full decay of the FID. For selective operation on the $(\frac{1}{2},-\frac{1}{2})$ transition for half-integer quadrupolar nuclei exhibiting large quadrupole coupling interactions the pulse flip angles are scaled by $(I + \frac{1}{2})^{-1}$ relative to the nominal flip angles written above the pulses. Rotor synchronization requires $\tau_1 = \tau_r - \tau_{\pi/2}$ and $2N\tau_r = \tau_a + 2\tau_2 + \tau_\pi$, where N is an integer, τ_r is the rotor period, and $\tau_{\pi/2}$ and τ_π are the durations of selective $\pi/2$ and π pulses.

$\tau_{\pi/2}$ and adjustment of the duration of the repeating unit according to $2N\tau_r = \tau_a + 2\tau_2 + \tau_\pi$, where N is an integer, $\tau_r = 2\pi/\omega_r$ is the rotor period, τ_2 is a delay preventing sampling close to the RF pulse, and $\tau_{\pi/2}$ and τ_π are the widths of the selective $\pi/2$ and π pulses. In the regime of large C_Q values relative to the amplitude $\omega_{RF}/2\pi$ of the RF irradiation, i.e., $2\pi C_Q/(4I(2I-1)\omega_{RF}) > 3$, the pulse sequence is tuned for selective operation on the $(\frac{1}{2},-\frac{1}{2})$ transition by scaling of the pulse flip angles according to $\theta_{1/2,-1/2} = \theta/(I + \frac{1}{2})$, where θ is the nominal pulse flip angle (*27–29*). The RF pulse phases θ_i (i = 1, 2, and 3) and the receiver reference phase are cycled to select the $p = 0 \rightarrow \pm 1 \rightarrow \mp 1 \rightarrow \pm 1$, etc., coherence transfer pathway (*16, 30*). Under these conditions the combined effect of the rotor and spin echoes of the QCPMG-MAS pulse sequence splits the second-order central transition lineshape into a number of spinning (rotary) sidebands, typical for standard MAS or QE MAS experiments, each of which are split into a manifold of equidistant spin-echo sidebands separated by the inverse of the effective spin-echo period, i.e., $1/\tau_a$.

Concentration of the overall spectral intensity, initially distributed over the full second-order quadrupolar spinning sideband powder patterns, into a finite number of discrete spin-echo sidebands leads to a considerable increase in spectral sensitivity relative to experiments relying on MAS alone. This phenomenon bears a close resemblence to the sensitivity gain encountered by going from static powder to MAS NMR spectra in the case of typical first-order anisotropic interactions. It should be noted, however, that while the rotary echoes of the standard MAS experiment are formed by modulation of the spatial part of the nuclear spin Hamiltonian by sample rotation, the echoes causing the sensitivity gain focused on in this work result from *additional* manipulation of the spin part of the Hamiltonian by a train of selective π pulses. The actual sensitivity gain and the ''digitilization'' of the envelope of the rotary sidebands containing the information on the anisotropic interaction parameters may be specified experimentally by adjusting the integral number of rotor echoes within each spin-echo period τ_a.

To demonstrate the performance of the QCPMG-MAS experiment, Fig. 2 compares ^{87}Rb ($I = \frac{3}{2}$) spectra of the two central transitions for Rb_2SO_4 corresponding to standard QE-MAS and QCPMG-MAS experiments. The experimental spectra were recorded on a Varian UNITY-400 spectrometer (9.4 T, 130.8 MHz for ^{87}Rb) using a homebuilt high-speed MAS probe (*31*) with a 5-mm Si_3N_4 rotor. The experiments used a spinning frequency $\omega_r/2\pi$ = 13,645 Hz and for the QCPMG-MAS experiment the spin-echo parameters were adjusted to split the second-order spinning sideband powder patterns into spin-echo sidebands separated by 250 Hz. In this case the QCPMG-MAS experiment provides a gain in signal intensity by a factor of 7 relative to the standard QE-MAS experiment while the essential features of the original centerband and spinning sideband lineshapes for the two rubidium sites in Rb_2SO_4 are clearly maintained as envelopes of spin-echo sidebands. Obviously, the sensitivity can be increased further at the expense of details in the spectral envelope. In addition to the direct gain in sensitivity, it is noted that the QCPMG-MAS experiment clearly facilitates discrimination of true sideband signals from noise/background as compared to the standard MAS or QE-MAS methods (see insets in Fig. 2).

X-ray diffraction shows that Rb_2SO_4 has orthorhombic crystal structure with space group *Pnam* (*32*) and thus has two magnetically nonequivalent rubidium sites in agreement with the spectra in Fig. 2. Parameters describing magnitudes and relative orientation of the quadrupole coupling and chemical shielding tensors for the two sites have previously been determined using static-powder QE (*5*), MAS (*8*), and single-crystal (*33*) NMR. It should be emphasized, however, that the weak chemical shielding interaction is easily averaged by MAS, implying that accurate information about this interaction and the relative tensor orientations in this case requires application of single-crystal NMR. Information about the anisotropic interactions (for high-speed MAS specifically the quadrupolar coupling) may be obtained from the sideband manifolds observed for the two sites in the QCPMG-MAS spectrum of Fig. 2b. This is demonstrated by the simulated MAS (or QE-MAS) and QCPMG-MAS spectra in Figs. 2c and 2d calculated using the parameters determined by single-crystal NMR (*33*) and under the assumption of ideal RF pulse performance. The MAS and QCPMG-MAS spectra were calculated on a Silicon Graphics Onyx computer using a MAS version of the software earlier described for the calculation of static-powder QCPMG spectra (*16*). Clearly, the simulated MAS and QCPMG-MAS

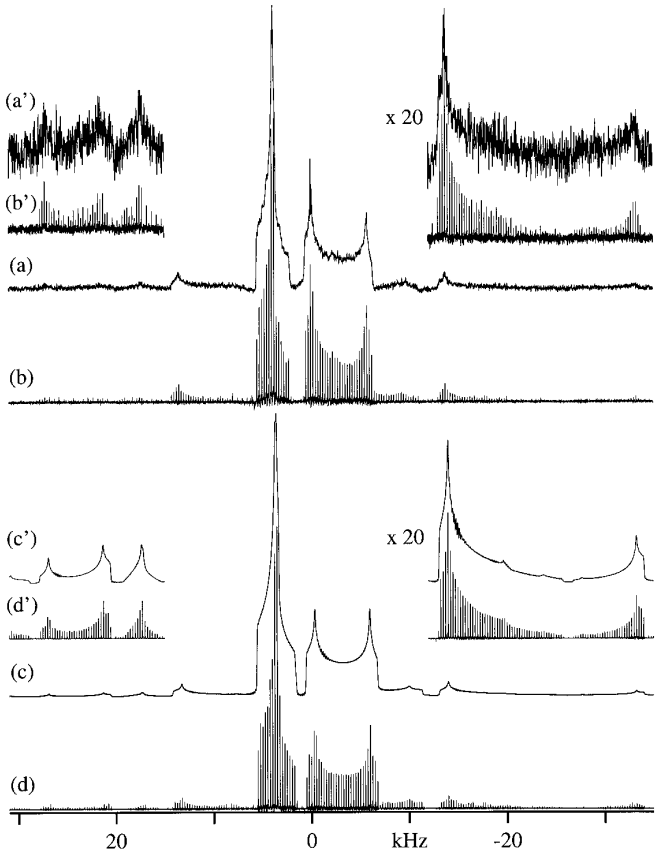

FIG. 2. ^{87}Rb (130.8 MHz) QE-MAS (a,c) and QCPMG-MAS (b,d) spectra of Rb_2SO_4 (purchased from Alfa Products, Karlsruhe, Germany, and used without further purification). The experimental spectra (a,b) were recorded using ω_r/π = 13,645 Hz, $\omega_{RF}/2\pi$ = 64.1 kHz (selective pulse widths of $t_{\pi/2} = t_\pi/2$ = 1.95 μs), τ_1 = 71.3 μs, τ_2 = 50.0 μs, τ_a = 4 ms (corresponding to 250 Hz spin-echo sideband separation), M = 19, τ_d = 3.92 ms, a spectral width of 100 kHz, 128 transients, and 4 s relaxation delay. The vertical scale of (b) is reduced by a factor of 7 relative to that in (a). (a′) and (b′) show vertical expansions of spinning sidebands from (a) and (b), respectively. The simulated spectra (c,d) and the corresponding expansion (c′,d′) were calculated using the above experimental parameters, apart from assuming ideal RF pulse performance. The following parameters were used for the magnitudes and relative orientations (shielding tensor relative to principal axis frame of the quadrupole coupling tensor) of the quadrupole coupling and chemical shielding tensors: C_Q = 2.72 MHz, η_Q = 0.93, σ_{iso} = 42.6 ppm, σ_{aniso} = 2.7 ppm, η_σ = 0.26, α^σ_{PC} = 76°, β^σ_{PC} = 17°, and γ^σ_{PC} = 110° for site 1 and C_Q = 5.29 MHz, η_Q = 0.12, σ_{iso} = 15.5 ppm, σ_{aniso} = −25.0 ppm, η_σ = 0.54, α^σ_{PC} = 9°, β^σ_{PC} = 37°, and γ^σ_{PC} = 270° for site 2 in accordance with Ref. (*33*). The chemical shift scale is referenced relative to external 1.0 M $RbNO_3$.

spectra, considering the second-order (secular part only) quadrupolar coupling interaction and vanishing effects from first-order chemical shielding, agree very well with respect to the envelope of the second-order spinning sideband powder patterns of the central transition. Minor discrepancies between the experimental and simulated spectra are ascribed to the effect of finite RF pulses which will be explored in more detail in a forthcoming study.

In conclusion, we have demonstrated that the QCPMG technique, recently proposed for sensitivity enhancement of static-powder spectra (*16*), may advantageously be combined with fast MAS. The resulting spectra show significant sensitivity enhancements relative to standard MAS or QE-MAS spectra while maintaining sufficient spectral information to extract accurate parameters for the anisotropic interaction tensors. The actual sensitivity gain (here a factor of 7) may be increased considerably for larger quadrupole coupling interactions, where standard MAS experiments even for nuclei with high relative sensitivity and short longitudinal relaxation times (such as ^{87}Rb) become increasingly time demanding. Relying on detection of the central transition alone, it is anticipated that the QCPMG-MAS experiment is experimentally feasible even in the regime of very large quadrupolar coupling interactions. In this case, however, numerical analysis of the QCPMG-MAS spectra need consideration of finite RF pulse effects as will be described elsewhere.

ACKNOWLEDGMENTS

The use of the Varian UNITY-400 spectrometer, sponsored by Teknologistyrelsen, at the University of Aarhus Instrument Centre for Solid-State NMR Spectroscopy is acknowledged. Support of this research by equipment grants from the Danish Natural Science Foundation Council, Carlsbergfondet, and Aarhus University Research Foundation is acknowledged. This work has been supported in part by the National Institutes of Health under a Related Services Agreement with the U.S. Department of Energy (DOE) under Contract DE-AC06-76RLS1830, Federal Grant 8-R1GM26295F. Pacific Northwest National Laboratory is operated for DOE by Batelle.

REFERENCES

1. J. Skibsted, N. C. Nielsen, H. Bildsøe, and H. J. Jakobsen, *Chem. Phys. Lett.* **188,** 405 (1992); *J. Am. Chem. Soc.* **115,** 7351 (1993).
2. J. Skibsted, T. Vosegaard, H. Bildsøe, and H. J. Jakobsen, *J. Phys. Chem.* **100,** 14872 (1996).
3. J. F. Baugher, P. C. Taylor, T. Oja, and J. P. Bray, *J. Chem. Phys.* **50,** 4914 (1969).
4. W. P. Power, R. E. Wasylishen, S. Mooibroek, B. A. Pettitt, and W. Danchura, *J. Phys. Chem.* **94,** 591 (1990).
5. J. T. Cheng, J. C. Edwards, and P. D. Ellis, *J. Phys. Chem.* **94,** 553 (1990).
6. J. Hirschinger, P. Granger, and J. Rose, *J. Phys. Chem.* **96,** 4815 (1992).
7. T. Vosegaard, J. Skibsted, H. Bildsøe, and H. J. Jakobsen, *J. Phys. Chem.* **99,** 10731 (1995).
8. C. Fernandez, J. P. Amoureux, P. Bodart, and A. Maijanen, *J. Magn. Reson.* A **113,** 205 (1995).
9. M. Bloom and E. Sternin, *Biochemistry* **26,** 2101 (1987).
10. J. T. Cheng and P. D. Ellis, *J. Phys. Chem.* **93,** 2549 (1989).
11. H. Y. Carr and E. M. Purcell, *Phys. Rev.* **94,** 630 (1954).
12. S. Meiboom and D. Gill, *Rev. Sci. Instrum.* **29,** 688 (1958).
13. I. Solomon, *Phys. Rev.* **110,** 61 (1958).
14. I. D. Weisman and L. H. Bennett, *Phys. Rev.* **181,** 1341 (1969).

15. J. H. Davis, K. R. Jeffrey, M. Bloom, M. I. Valic, and T. P. Higgs, *Chem. Phys. Lett.* **42,** 390 (1976).

16. F. H. Larsen, H. J. Jakobsen, P. D. Ellis, and N. C. Nielsen, *J. Phys. Chem.* A **101,** 8597 (1997).

17. A. N. Garroway, *J. Magn. Reson.* **28,** 365 (1977).

18. A. J. Vega, *J. Magn. Reson.* **65,** 252 (1985).

19. S. Swanson, S. Ganapathy, S. Kennedy, P. M. Henrichs, and R. G. Bryant, *J. Magn. Reson.* **69,** 531 (1986).

20. M. Engelsberg and C. S. Yannoni, *J. Magn. Reson.* **88,** 393 (1990).

21. K. Müeller, R. Poupko, and Z. Luz, *J. Magn. Reson.* **90,** 19 (1990).

22. M. J. Lizak, T. Gullion, and M. S. Conradi, *J. Magn. Reson.* **91,** 254 (1991).

23. P. S. Marchetti, L. Bhattacharyya, P. D. Ellis, and C. F. Brewer, *J. Magn. Reson.* **80,** 417 (1988).

24. S. Bank, J. F. Bank, and P. D. Ellis, *J. Phys. Chem.* **93,** 4847 (1989).

25. P. M. Henrichs and V. A. Nicely, *Macromolecules* **24,** 2506 (1991).

26. A. Samoson, E. Kundla, and E. Lippmaa, *J. Magn. Reson.* **49,** 350 (1982).

27. A. Abragam, ''The Principles of Nuclear Magnetism,'' Clarendon Press, Oxford (1961).

28. V. H. Schmidt, *in* ''Proceedings, Ampère Intl. Summer School II,'' p. 79, 1971.

29. N. C. Nielsen, H. Bildsøe, and H. J. Jakobsen, *Chem. Phys. Lett.* **191,** 205 (1992); *J. Magn. Reson.* **97,** 149 (1992).

30. M. Rance and A. Byrd, *J. Magn. Reson.* **52,** 221 (1983).

31. H. J. Jakobsen, P. Daugaard, and V. Langer, *J. Magn. Reson.* **76,** 162 (1988).

32. A. G. Nord, *Acta Crystallogr. Sect. B* **30,** 1640 (1974).

33. T. Vosegaard, J. Skibsted, H. Bildsøe, and H. J. Jakobsen, *J. Magn. Reson.* A **122,** 111 (1996).